

1 John R. Worden¹, Susan S. Kulawik², Dejian Fu¹, Vivienne H. Payne¹, Alan E. Lipton³, Igor
2 Polonsky³, Yuguang He³, Karen Cady-Pereira³, Jean-Luc Moncet³, Robert L. Herman¹, Frederick
3 W. Irion¹, and Kevin W. Bowman¹

4
5 1. Jet Propulsion Laboratory / California Institute for Technology, Pasadena, CA

6 2. Bay Area Environmental Research Institute, Mountain View CA, USA

7 3. Atmospheric Environmental Research, Lexington MA, USA

8

9 **Characterization and Evaluation of AIRS-Based Estimates of the Deuterium Content of**
10 **Water Vapor**

11

12 **Abstract:** Single pixel, tropospheric retrievals of HDO and H₂O concentrations are retrieved
13 from Atmospheric Infrared Sounder (AIRS) radiances using the optimal estimation algorithm
14 developed for the Aura Tropospheric Emission Spectrometer (TES) project. We evaluate the
15 error characteristics and vertical sensitivity of AIRS measurements corresponding to five days of
16 TES data (or 5 global surveys) during the Northern Hemisphere summers between 2006 and
17 2010 (~600 co-located comparisons per day). We find that the retrieval characteristics of the
18 AIRS deuterium content measurements have similar vertical resolution in the middle-troposphere
19 as TES but with slightly less sensitivity in the lower-most troposphere, with a typical degrees-of-
20 freedom (DOFS) in the tropics of 1.5. The calculated measurement uncertainty is ~30 per mil
21 (parts per thousand relative to the deuterium composition of ocean water) for a tropospheric
22 average between 750 and 350 hPa, the altitude region where AIRS is most sensitive, as
23 compared to ~15 per mil for the TES data. Comparison with the TES data also indicate that the
24 uncertainty of a single target AIRS HDO/H₂O measurement is ~30 per mil. Comparison of AIRS
25 and TES data between 30 degrees South and 50 degrees North indicate that the AIRS data is
26 biased low by ~-2.6 per mil with a latitudinal variation of ~-7.8 per mil. This latitudinal variation
27 is consistent with the accuracy of TES data as compared to in situ measurements, suggesting that
28 both AIRS and TES have similar accuracy.

29

30 © 2019. All rights reserved.

31

32

33

1 **Introduction:**

2 Measurements of the isotopic composition of water can help identify the source of the
3 water and provide knowledge about its condensation and evaporation history (e.g. Galewsky *et*
4 *al.* and refs therein). Through most of the twentieth century, most isotopic measurements of
5 water have been of precipitation (e.g. Craig, 1961). Near global measurements of the isotopic
6 composition of water vapor became possible with the advent of spectroscopic techniques applied
7 to in situ measurements (e.g., Noone *et al.*, 2011) using lasers and for passive ground based and
8 satellite measurements (e.g. Worden *et al.*, 2006; Frankenberg *et al.* 2009; Schneider *et al.* 2012;
9 Lacour *et al.* 2012). These data have in turn been used to evaluate the role of convection, large
10 scale dynamics, and evapotranspiration on the tropical water cycle (e.g. Worden *et al.* 2007;
11 Frankenberg *et al.* 2009; Wright *et al.* 2017) tropical convection (e.g. Lacour 2018 and refs
12 therein) and the role of plants on global evapotranspiration (Good *et al.* 2015).

13 In this paper we demonstrate a retrieval algorithm, based upon the Aura TES optimal
14 estimation retrieval algorithm (e.g. Worden *et al.* 2012) that can provide robustly characterized
15 measurements of the deuterium content of water vapor (HDO and H₂O) from the AIRS
16 measurements. Our goal is to create a multi-decadal Earth Science Data Record (ESDR) using
17 the AIRS and TES data; the TES global record spans ~6 years (2005-2010) and the AIRS data
18 span 17+ years starting in 2002. This ESDR could potentially be used for evaluating the
19 changing water cycle (e.g. Bailey *et al.*, 2017) and its coupling to the carbon cycle (e.g. Zhou *et*
20 *al.*, 2014; Wright *et al.*, 2017).

21 We first characterize the vertical resolution and uncertainties for estimates of HDO and
22 H₂O, and their ratio, using AIRS radiance observations corresponding to boreal summertime TES
23 global survey's between 2006 through 2010, which is the time period when TES observations
24 sample the (near) global atmosphere and the calibration approach for TES measurements
25 remained the same. We make only these comparisons due to current processing limitations but
26 expect additional overlap between TES and AIRS data sets in the coming years. We then
27 compare the AIRS and TES data to evaluate the calculated uncertainties of the AIRS data.

28

29 **1) Description of AIRS and TES instruments**

30

31 The AIRS instrument is a nadir-viewing, scanning infrared spectrometer (Aumann *et al.*
32 2003; Pagano *et al.*, 2003; Irion *et al.* 2018; DeSouza-Machado *et al.* 2018) that is onboard the

1 NASA Aqua satellite and was launched in 2002. AIRS measures the thermal radiance between
2 approximately 3-12 microns with a resolving power of approximately 1200. For the 8 micron
3 spectral range used for the HDO/H₂O retrievals, the spectral resolution is $\sim 1 \text{ cm}^{-1}$ with a gridding
4 of $\sim 0.5 \text{ cm}^{-1}$; the signal-to-noise (SNR) ranges from ~ 400 to ~ 1000 over the 8 micron region for a
5 typical tropical scene. A single footprint has a diameter of $\sim 15 \text{ km}$ in the nadir; with the ~ 1650
6 km swath, the AIRS instrument can measure nearly the whole globe in a single day. The Aqua
7 satellite is part of the “A-Train” that consists of multiple satellites, including TES, in a sun-
8 synchronous orbit at 705 km with an approximately 1:30 pm equator crossing-time.

9 The Aura TES instrument is a Fourier Transform Spectrometer that originally was
10 designed to measure the thermal infrared (IR) radiances both in the limb and nadir viewing in
11 order to obtain vertically resolved trace gas profiles of ozone, CO, CH₄, HDO and H₂O, and
12 several ozone pre-cursors such as ammonia, methanol, and PAN (e.g. Beer *et al.*, 2001; Worden
13 *et al.*, 2004; Worden *et al.* 2006; Luo *et al.*, 2007; Beer *et al.* 2008; Worden *et al.*, 2012; Payne *et al.*
14 *et al.* 2014). Several of these trace gases, such as CO, CH₄, and ammonia have also been quantified
15 using AIRS radiances (e.g. McMillan *et al.*, 2005; Xiong *et al.* 2008; Warner *et al.*, 2016). In
16 comparison to the AIRS instrument, TES has a spectral resolution of $\sim 0.12 \text{ cm}^{-1}$ (apodized) with
17 a spectral gridding of 0.06 cm^{-1} . The SNR is ~ 300 in the 8 microns spectral region. The Aura TES
18 instrument, after the summer of 2005, observes one nadir scene every 100 km along the orbit
19 path. The effective length of the record is approximately five years, between September 2005
20 through November 2009, after which instrument degradation problems resulted in interrupts and
21 a decrease in sampling. The AIRS instrument has nearly one thousand times the sampling of TES
22 and near continuous operation between 2002 through the present and therefore can be used to
23 construct several composition based ESDR’s.

24

25 **3) Description of the Radiative Transfer Forward Model**

26

27 The radiative transfer forward model used for this work is the Optimal Spectral Sampling
28 (OSS) fast radiative transfer model (RTM) (Moncet *et al.*, 2015; Moncet *et al.*, 2008). The OSS
29 approach is integrated in the operational Cross-Track Infrared Sounder (CrIS, Han *et al.* 2013)
30 processing system (Divarkala *et al.*, 2014) and has also been utilized for trace gas retrievals from
31 CrIS (e.g. Shephard and Cady-Pereira, 2015). OSS uses a series of approximations tailored to a

1 specific frequency range and spectral resolution to increase the radiative transfer calculation
2 performance by approximately a factor of 20-100 relative to a line-by-line calculation
3 (<http://rtweb.aer.com>). OSS can be trained to user-defined accuracy relative to the line-by-line
4 model used for training. Here, the training threshold was set to 20 % of the AIRS noise level.
5 The line-by-line model used as a reference in the training and to build the absorption coefficient
6 look-up tables (LUTs) used by the fast RTM is the Line-By-Line Radiative Transfer Model
7 (LBLRTM) (Clough et al., 2005; Alvarado et al., 2013). The OSS version used in this work is
8 based on LBLRTM v12.4, using the TES_v2.0 spectroscopic line parameter database. The
9 TES_v2.0 line parameter database follows the HITRAN 2012 compilation (Rothman et al.,
10 2013]), with the following exceptions:

- 11 • H₂O positions and intensities are taken from the aer_v_3.4 line parameter database
12 (<http://rtweb.aer.com>), closely following the measured and calculated values published in
13 Coudert et al. (2008).
- 14 • CH₄ includes first order line mixing coefficients (as supplied in the aer_v_3.4 line
15 parameter database). These were calculated using the approach of Tran et al. (2006).
- 16 • CO₂ line parameters are from the database of Lamouroux et al. (2015). This database
17 takes most of its line positions, intensities, and lower state energies from the HITRAN
18 2012 database, but the values for air-broadening half-widths and their temperature
19 dependences are adjusted from the HITRAN 2012 values to be consistent
20 throughout the bands, and the air-induced pressure shifts (not given for a majority of
21 transitions in HITRAN 2012) were added. The TES_v2.0 database includes first order
22 line mixing coefficients (as supplied in the aer_v_3.4.1 line parameter database),
23 calculated using the software of Lamouroux et al. (2015).

24 Further information on the AER line parameter databases can be found at <http://rtweb.aer.com>.
25 OSS is adapted for use with AIRS radiances using the version 4 AIRS spectral response function
26 (SRF) (Strow et al., 2003) that is interpolated to a uniform grid of 0.004 cm⁻¹ centered on the
27 channel center frequencies. The OSS radiative transfer code provides speedup of 20-100x over
28 the original TES operational radiation transfer model (Clough *et al.*, 2006).

29

30 **4) Description of the Retrieval Approach**

1
2
3
4
5
6
7
8
9
10
11
12
13
14
15
16
17
18
19
20
21
22
23
24
25
26
27
28
29
30
31

The optimal estimation algorithm used in this analysis for quantifying CH₄, HDO, H₂O, temperature, cloud properties, and emissivity is extensively discussed in Worden et al. (2004), Bowman et al. (2006), and Worden et al (2012). We therefore refer the reader to those papers for a description of the retrieval algorithm, with a suggestion that they start with the Worden *et al.* (2012) paper; however, we will briefly summarize the retrieval approach here. This retrieval algorithm, now called the MUlti-SpEctra, MUlti-SpEcies, MUlti-Sensors (MUSES) algorithm (Worden et al., 2007b; Fu et al., 2013, 2016, 2018; Luo et al., 2013; Worden et al., 2013), can use radiances from multiple instruments including TES, CrIS, OMI, OMPS, TROPOMI, and MLS to quantify geophysical observables that affect the corresponding radiance.

For the AIRS retrievals discussed here, we simultaneously estimate not just CH₄, CO, HDO, and H₂O but also temperature (surface and atmosphere), emissivity (if over land), and a spectrally varying gray body cloud (e.g. Kulawik *et al.*, 2006, Eldering *et al.*, 2008). As in Worden *et al.* (2006) and Worden *et al.* (2012) the constraint matrix used to regularize the HDO and H₂O components of the retrieval includes off-diagonal components that reflect *a priori* knowledge about the variability of HDO with respect to H₂O in order to ensure that retrieval of the ratio of HDO to H₂O is optimized, as opposed to either HDO or H₂O alone. The prior information used for this covariance is derived from monthly climatologies using the NCAR Global Climate Model as discussed in Worden *et al.* (2006). The *a priori* profile used for the HDO/H₂O ratio is set to be constant over the whole globe, and represents the mean tropical *a priori* profile from the NCAR model. However, the H₂O *a priori* profile is allowed to vary by latitude and is based on re-analysis (Worden *et al.* 2006); therefore the HDO profile is the mean tropical profile of the HDO/H₂O ratio from the NCAR model multiplied by the H₂O *a priori* profile.

We use single pixel radiances that have not been transformed through “cloud clearing” in order to preserve the original, well characterized radiance noise characteristics for use in our estimates (Irion *et al.* 2018; DeSouza-Machado *et al.* 2018) and because we find that single-pixel AIRS radiances have sufficient information about cloud pressure and optical depth to be retrieved jointly with the trace gases, as demonstrated empirically through validation of these AIRS-based composition retrievals with TES retrievals (e.g. Figures 1-4). We assume the noise in any given pixel is uncorrelated with those from adjacent pixels. However, these correlations

1 are known to exist (e.g. Pagano *et al.* 2008) and the impact of ignoring them is that our
2 calculated uncertainties will be larger than expected and therefore our noise related uncertainty
3 should be considered a conservative estimate.

4 A primary difference between the retrieval approach shown in this paper versus the TES
5 methane and HDO retrievals (Worden *et al.*, 2012) and those from previous efforts using AIRS
6 radiances (e.g. Xiong *et al.*, 2008) is that we retrieve these trace gas profiles using the AIRS
7 radiances from ~ 8 and ~ 12 microns instead of radiances from the 8 micron region alone in order
8 to provide a stronger constraint on atmospheric temperature and hence reduce uncertainty from
9 knowledge of temperature on the HDO and H₂O retrieval. The 8 micron region used (~ 1217 to
10 1315 cm⁻¹) for these retrievals has the most sensitivity to HDO and H₂O whereas the 12 micron
11 band (~ 650 to 900 cm⁻¹) is primarily sensitive to temperature and H₂O. All channels are used
12 within this spectra unless flagged as poor during calibration.

13

14 **5) Characterization of HDO/H₂O profiles**

15

16 While H₂O is quantified using radiances from both the 12 micron and 8 micron spectral
17 regions, the primary absorption lines used here to quantify HDO are in the 8 micron region.
18 There are other HDO (and H₂O) lines available to use from the AIRS radiance but for now we
19 only use the 8 micron region to ensure consistency between AIRS and TES data. Figure 1 shows
20 the 8 micron radiance (top panel) and the Jacobian, or sensitivity of the radiance to variations in
21 the (log) H₂O and (log) HDO respectively (middle and bottom panels). These Jacobians are
22 normalized by the instrument noise. For example, a value of 1 means that it would take a 100%
23 change in the corresponding species to distinguish between two similar radiances (everything
24 about the observed scene and radiance is the same except for the species of interest) above the
25 noise level. A value of ~ 50 therefore means that only a 2% variation is required (or 1/50).

26 Figure 2 shows the averaging kernel matrix for the HDO component of the joint retrieval.

27 The averaging kernel describes the response of the estimate, or log(HDO), relative to variations
28 in the true state; consequently it can also be used to evaluate the vertical resolution and
29 sensitivity of the estimate. For example, if HDO varies by 100% at 908 hPa, then the AIRS
30 estimate would be able to observe about 30% of the variability because the averaging kernel is
31 approximately 0.3 at that level. The averaging kernel at 908 hPa also depends on the deuterium

1 content at several other pressure levels below and above indicating that the estimate at 908 hPa
2 depends on the deuterium content variations at these other levels. Not shown are the
3 dependencies of the (log) HDO estimate to those from the (log) H₂O estimate. These
4 dependencies between the HDO averaging kernels and with the H₂O averaging kernels are
5 accounted for when constructing the HDO/H₂O ratio; however a residual uncertainty called the
6 “smoothing” error is imparted when comparing the HDO/H₂O ratio to independent data; this
7 smoothing error is part of the error budget shown in Figure 3. As discussed in Worden *et al.*
8 (2012) and Schneider *et al.* (2012), the sensitivity of the estimated HDO/H₂O ratio is limited by
9 the sensitivity of the estimate to HDO. Users of these data should note that this ratio is typically
10 used with that of H₂O in order to better evaluate their joint variation (HDO/H₂O, H₂O) against
11 simple mixing and rainfall models (Noone *et al.* 2011). However, the sensitivity of the radiance
12 to H₂O variations is much stronger than that for HDO, although the altitude region of the HDO
13 sensitivity typically overlaps with the H₂O sensitivity. Schneider *et al.* (2012) discusses how to
14 created HDO/H₂O, H₂O pairs to mitigate this component of the smoothing error when comparing
15 these data against the simple models described in Noone *et al.* (2011). For comparison to more
16 complex global climate models the user of these data also needs to apply the HDO and H₂O
17 averaging kernels to the corresponding model fields (e.g. Risi *et al.*, 2012).

18 Figure 3 (top panel) shows the tropospheric deuterium content (or HDO/H₂O ratio)
19 derived from AIRS observations on July 1 2006. Despite the improved computational
20 performance of the OSS radiative transfer calculation relative to the TES algorithm line-by-line
21 calculation (Clough *et al.* 2005), the retrieval is still sufficiently expensive such that we can only
22 process a sub-set of the AIRS retrievals. Considering the computational cost, for the purpose of
23 constructing a record we currently only process AIRS retrievals from between 45 degrees South
24 to 65 degrees North that coincide with the nearest TES observation but with an additional two
25 observations within 100 km of the TES track over the continents; this ad hoc sampling strategy is
26 based on experience with previous studies using the TES deuterium and methane measurements.
27 The traditional notation for this quantity is called “delta-D” , or “ δ -D” with units of “per mil” or
28 parts per thousand relative to the Standard Mean Ocean Water (SMOW) deuterium content
29 which is 3.11×10^{-4} molecules of HDO per molecule of H₂O. The observations shown represent
30 the deuterium content for the pressures between 750 hPa and 350 hPa, where we find the AIRS
31 and TES observations have maximal overlap in their vertical resolution.

1 The errors are calculated during the optimal estimation retrieval (Bowman *et al.* 2007;
2 Worden *et al.* 2012) and depend on the expected noise of the AIRS radiances and the parameters
3 that are co-retrieved with the AIRS HDO/H₂O ratio such as temperature, surface emissivity,
4 clouds, and methane. As noted in Worden *et al.* (2012) these co-retrieved parameters affect both
5 the precision and accuracy whereas the noise only affects the precision. The total error (middle
6 panel) is given in units of per mil and ranges between 25 to 30 per mil. The DOFS, or trace of
7 the averaging kernel, are shown in the bottom panel and indicate that many of the HDO/H₂O
8 retrievals can resolve different parts of the troposphere, at least in the tropics, because (as
9 demonstrated in Figure 2) the rows of the averaging kernels are separated between the boundary
10 layer region (surface to ~750 hPa) and the free-troposphere (~600 to 300 hPa). However, these
11 observations cannot completely resolve the total variability in these two regions of the
12 atmosphere because the total DOFS is typically 1.5 or less and for the measurement to be able to
13 resolve the variability (to within the calculated error) of the two regions there would need to be
14 at least 2 DOFS.

15

16 **6) Comparison of AIRS and TES HDO/H₂O retrievals**

17

18 Figure 4 shows a comparison between overlapping AIRS and TES estimates of the
19 HDO/H₂O ratio for June 1 2006. The AIRS and TES measurements effectively overlap in space
20 and within a few seconds in time as the instruments are in the same orbit. However not all the
21 comparisons shown in Figure 4 overlap as retrievals may be rejected due to poor quality. We
22 therefore compare all data that are within 200 km in the free troposphere. We do not expect
23 substantive error to occur due to spatial mismatch of 2 degrees or less because air parcels in the
24 free-troposphere have length scales that are several hundred kilometers long (e.g. Worden *et al.*
25 2013). The average between approximately 750 hPa and 350 hPa are shown for when the DOFS
26 are larger than one for this altitude region. There is a slight bias of -2.7 +/- 1.5 per mil between
27 TES and AIRS as shown in the top panel. The calculated and actual (RMS difference between
28 AIRS and TES) uncertainties are shown and are approximately 30 per mil, primarily driven by
29 the uncertainty in the AIRS based estimates as the TES based estimates have an uncertainty of
30 approximately 15 per mil. Figure 5 shows a direct comparison of the AIRS and TES data. The
31 correlation is about 0.89 and the one-to-one line (solid line) overlaps this distribution. However

1 the lowest values likely diverge from the one-to-one line, possibly because the vertical
2 distribution in the sensitivity depends on the amount of HDO and hence we should expect
3 differences between the TES and AIRS deuterium measurements for these lower-sensitivity
4 retrievals.

5 A comparison of the AIRS and TES HDO/H₂O ratio for five single global surveys taken
6 between 2006 and 2010 (one global survey per year during boreal summer) is shown in Table 1
7 and indicates that the overall bias varies between -2.7 to 3.7 per mil. Using all 5 TES global
8 surveys that are summarized in Table 1 we can construct how AIRS and TES compare as a
9 function of latitude as shown in Figure 6. Figure 6 is constructed by averaging the difference
10 between TES and AIRS observations within 5 degree latitudinal bins. The mean bias across
11 latitudes is ~-2.6 per mil. The error bars shown on the difference is the error on the mean, which
12 is the Root-Mean-Square (RMS) of the differences divided by the square root of the number of
13 co-located observations; as this error bar is a measure of precision for each latitude bin, this
14 comparison demonstrates that there are variations in the comparison that are larger than the
15 precision and are therefore related to systematic errors in either the TES data or AIRS data or
16 both. Variations in these systematic errors can be seen in the latitudinal variability, which has an
17 RMS variation of ~7.8 per mil for the different latitude bins but can vary by as much as ~-15 to
18 ~+15 per mil in the tropics. Typically these variations are due to a combination of uncertainties
19 in the spectroscopy along with temperature, water vapor, and surface properties; they may also
20 be due to “smoothing error” which is related to how differences in the vertical resolution affect
21 the tropospheric average of the deuterium content shown in these figures (e.g. Worden *et al.*
22 2004). This 7.8 per mil variation across latitudes is about the same as the reported accuracy of
23 the Aura TES delta-d observations that are based on comparisons of TES data with surface and
24 aircraft measurements (Worden *et al.* 2011; Herman *et al.* 2014). We therefore report the current
25 accuracy of the AIRS data to be ~7.8 per mil. We expect future comparisons between these data
26 and those from aircraft or revisions to the AIRS retrieval approach will modify this estimate of
27 the accuracy.

28
29

30 **8) Conclusion**

31

1 This paper describes the vertical resolution and error characteristics of retrievals of the
2 deuterium content (or the HDO/H₂O ratio) of water vapor using AIRS radiances and then
3 evaluates the consistency between AIRS and TES retrievals of HDO and H₂O. We find that the
4 AIRS and TES deuterium content for the lower-troposphere (750 – 350 hPa) are consistent, or
5 within their calculated uncertainties, for the 5 year period in which TES observations span the
6 globe (2006-2010). We find the total uncertainty for a single AIRS observation is ~30 per mil
7 with an accuracy of ~7.8 per mil. These uncertainties can be compared to the observed total
8 variability, which can range from approximately -350 to -50 per mil over the whole globe, as
9 observed by the Aura TES data (Worden *et al.* 2006) and shown in Figure 3 for AIRS data.

10 While only five days of comparisons are shown here for the purpose of evaluating the
11 retrieval approach and error characteristics of these AIRS retrievals, we expect to produce a
12 record of the AIRS-based deuterium content retrievals from the start of the mission (2002)
13 through the present. Because of computational limitations, we expect to process data from 45
14 degrees South to 65 degrees North at approximately four times the sampling of the Aura TES
15 measurements and with increased sampling (~3x) over the continental regions with the goal of
16 increasing this sampling once the initial record is completed and as additional resources become
17 available.

18

19

20 **Acknowledgements**

21

22 The research was carried out at the Jet Propulsion Laboratory, California Institute of
23 Technology, under a contract with the National Aeronautics and Space Administration.
24

1 **References**

- 2 Alvarado, M. J., Payne, V. H., Mlawer, E. J., Uymin, G., Shephard, M. W., Cady-Pereira, K. E.,
3 Delamere, J. S. and Moncet, J. L.: Performance of the Line-By-Line Radiative Transfer Model
4 (LBLRTM) for temperature, water vapor, and trace gas retrievals: recent updates evaluated with
5 IASI case studies, *Atmospheric Chemistry and Physics*, 13(14), 6687–6711, doi:10.5194/acp-13-
6 6687-2013-supplement, 2013.
- 7
- 8 Aumann, H. H., Chahine, M. T., Gautier, C., Goldberg, M. D., Kalnay, E., McMillin, L. M.,
9 Revercomb, H., Rosenkranz, P. W., Smith, W. L., Staelin, D. H., Strow, L. L. and Susskind, J.:
10 AIRS/AMSU/HSB on the aqua mission: design, science objectives, data products, and
11 processing systems, *IEEE TRANSACTIONS ON GEOSCIENCE AND REMOTE SENSING*,
12 41(2), 253–264, doi:10.1109/TGRS.2002.808356, 2003.
- 13
- 14 Bailey, A., Blossey, P. N., Noone, D., Nusbaumer, J. and Wood, R.: Detecting shifts in tropical
15 moisture imbalances with satellite-derived isotope ratios in water vapor, *Journal of Geophysical*
16 *Research-Atmospheres*, 122(11), 5763–5779, doi:10.1029/2010JD015197, 2017.
- 17
- 18 Beer, R., Glavich, T. A. and Rider, D. M.: Tropospheric emission spectrometer for the Earth
19 Observing System’s Aura satellite, *Applied optics*, 40(15), 2356–2367, 2001.
- 20
- 21 Beer, R., Shephard, M. W., Kulawik, S. S., Clough, S. A., Eldering, A., Bowman, K. W., Sander,
22 S. P., Fisher, B. M., Payne, V. H., Luo, M., Osterman, G. B. and Worden, J. R.: First satellite
23 observations of lower tropospheric ammonia and methanol, *Geophysical Research Letters*, 35(9),
24 L09801, doi:10.1029/2008GL033642, 2008.
- 25
- 26 Bowman, K. W., Rodgers, C. D., Kulawik, S. S., Worden, J., Sarkissian, E., Osterman, G., Steck,
27 T., Lou, M., Eldering, A. and Shephard, M.: Tropospheric emission spectrometer: Retrieval
28 method and error analysis, *IEEE TRANSACTIONS ON GEOSCIENCE AND REMOTE*
29 *SENSING*, 44(5), 1297–1307, 2006.
- 30
- 31 Clough, S. A., M. W. Shephard, E. J. Mlawer, J. S. Delamere, M. J. Iacono, K. Cady-Pereira, S.
32 Boukabara, and P. D. Brown: Atmospheric radiative transfer modeling: A summary of the AER
33 codes. *J. Quant. Spectroscopic. Radiative Transfer*, 91, 233–244, doi:
34 10.1016/j.jqsrt.2004.05.058, 2005
- 35
- 36 Clough, S. A., Shephard, M. W., Worden, J., Brown, P. D., Worden, H. M., Luo, M., Rodgers,
37 C. D., Rinsland, C. P., Goldman, A. and Brown, L.: Forward model and Jacobians for
38 tropospheric emission spectrometer retrievals, *IEEE TRANSACTIONS ON GEOSCIENCE*
39 *AND REMOTE SENSING*, 44(5), 1308–1323, 2006.
- 40
- 41 Craig, H.: Isotopic variations in meteoric waters, *Science*, 133, 1702–1703, 1961.
- 42
- 43 Coudert, L., Wagner, G., Birk, M., Baranov, Y.I., Lafferty, W.J., [Flaud](#), J-M.: The (H₂O)-O-16
44 molecule: Line position and line intensity analyses up to the second triad, *Journal Molecular*
45 *Spectroscopy*, **251**, 339-357, 2008
- 46

1 DeSouza-Machado, S., Strow, L. L., Tangborn, A., Huang, X., Chen, X., Liu, X., Wu, W. and
2 Yang, Q.: Single-footprint retrievals for AIRS using a fast Two Slab cloud-representation model
3 and the SARTA all-sky infrared radiative transfer algorithm, *Atmospheric Measurement*
4 *Techniques*, 11(1), 529–550, doi:10.1029/2005GL023211, 2018.

5
6 Divakarla, M. G., and Coauthors: The CrIMSS EDR algorithm: Characterization, optimization,
7 and validation. *J. Geophysical Research-Atmospheres*, 119, 4953–4977, doi:
8 10.1002/2013JD020438 (2014)

9
10 Eldering, A., Kulawik, S. S., Worden, J., Bowman, K. and Osterman, G.: Implementation of
11 cloud retrievals for TES atmospheric retrievals: 2. Characterization of cloud top pressure and
12 effective optical depth retrievals, *Journal of Geophysical Research-Atmospheres*, 113(D16),
13 D16S37, doi:10.1029/2007JD008858, 2008.

14
15 Frankenberg, C., Yoshimura, K., Warneke, T., Aben, I., Butz, A., Deutscher, N., Griffith, D.,
16 Hase, F., Notholt, J., Schneider, M., Schrijver, H. and Rockmann, T.: Dynamic Processes
17 Governing Lower-Tropospheric HDO/H₂O Ratios as Observed from Space and Ground,
18 *Science*, 325(5946), 1374–1377, doi:10.1126/science.1173791, 2009.

19
20 Frankenberg, C., Wunch, D., Toon, G., Risi, C., Scheepmaker, R., Lee, J.-E., Wennberg, P. and
21 Worden, J.: Water vapor isotopologue retrievals from high-resolution GOSAT shortwave
22 infrared spectra, *Atmospheric Measurement Techniques*, 6(2), 263–274, doi:10.5194/amt-6-263-
23 2013, 2013.

24
25 Fu, D., Kulawik, S. S., Miyazaki, K., Bowman, K. W., Worden, J. R., Eldering, A., Livesey, N.
26 J., Teixeira, J., Irion, F. W., Herman, R. L., Osterman, G. B., Liu, X., Levelt, P. F., Thompson,
27 A. M. and Luo, M.: Retrievals of tropospheric ozone profiles from the synergism of AIRS and
28 OMI: methodology and validation, *Atmospheric Measurement Techniques*, 11(10), 5587–5605,
29 doi:10.5194/amt-11-5587-2018-supplement, 2018.

30
31 Fu, D., Bowman, K. W., Worden, H. M., Natraj, V., Worden, J. R., Yu, S., Veeffkind, P., Aben,
32 I., Landgraf, J., Strow, L. and Han, Y.: High-resolution tropospheric carbon monoxide profiles
33 retrieved from CrIS and TROPOMI, *Atmospheric Measurement Techniques*, 9(6), 2567–2579,
34 doi:10.5194/amt-9-2567-2016-supplement, 2016.

35
36 Fu, D., Worden, J. R., Liu, X., Kulawik, S. S., Bowman, K. W. and Natraj, V.: Characterization
37 of ozone profiles derived from Aura TES and OMI radiances, *Atmospheric Chemistry and*
38 *Physics*, 13(6), 3445–3462, doi:10.5194/acp-13-3445-2013, 2013.

39
40 Galewsky, J., Larsen, H. S., Field, R. D., Worden, J. R., Risi, C. and Schneider, M.: Stable
41 isotopes in atmospheric water vapor and applications to the hydrologic cycle, *Rev. Geophys.*,
42 doi:10.1002/2015RG000512, 2016.

43
44 Good, S. P., Noone, D. and Bowen, G.: Hydrologic connectivity constrains partitioning of global
45 terrestrial water fluxes, *Science*, 349(6244), 175–177, doi:10.1126/science.aaa5931, 2015.

46

1 Han, Y., Revercomb, H., Crompton, M., Gu, D., Johnson, D., Mooney, D., Scott, D., Strow, L.,
2 Bingham, G., Borg, L., Chen, Y., DeSloover, D., Esplin, M., Hagan, D., Jin, X., Knuteson, R.,
3 Motteler, H., Predina, J., Suwinski, L., Taylor, J., Tobin, D., Tremblay, D., Wang, C., Wang, L.,
4 Wang, L. and Zavyalov, V.: Suomi NPP CrIS measurements, sensor data record algorithm,
5 calibration and validation activities, and record data quality, *Journal of Geophysical Research-*
6 *Atmospheres*, 118(22), 12,734–12,748, doi:10.1002/2013JD020457, 2013.
7
8 Herman, R. L., Cherry, J. E., Young, J., Welker, J. M., Noone, D., Kulawik, S. S. and Worden,
9 J.: Aircraft validation of Aura Tropospheric Emission Spectrometer retrievals of HDO / H₂O,
10 *Atmospheric Measurement Techniques*, 120, 3127–3138, doi:10.5194/amt-7-3127-2014, 2014.
11
12 Irion, F. W., Kahn, B. H., Schreier, M. M., Fetzer, E. J., Fishbein, E., Fu, D., Kalmus, P., Wilson,
13 R. C., Wong, S. and Yue, Q.: Single-footprint retrievals of temperature, water vapor and cloud
14 properties from AIRS, *Atmospheric Measurement Techniques*, 11(2), 971–995,
15 doi:10.1117/12.615244, 2018.
16
17 Kulawik, S. S., Worden, J., Eldering, A., Bowman, K., Gunson, M., Osterman, G. B., Zhang, L.,
18 Clough, S. A., Shephard, M. W. and Beer, R.: Implementation of cloud retrievals for
19 Tropospheric Emission Spectrometer (TES) atmospheric retrievals: part 1. Description and
20 characterization of errors on trace gas retrievals, *Journal of Geophysical Research-Atmospheres* ,
21 111, D24204, doi:10.1029/2005JD006733, 2006.
22
23 Kulawik, S. S., Bowman, K. W., Luo, M., Rodgers, C. D. and Jourdain, L.: Impact of
24 nonlinearity on changing the a priori of trace gas profile estimates from the Tropospheric
25 Emission Spectrometer (TES), *Atmospheric Chemistry Physics*, 8, 3081–3092, 2008.
26
27 Kulawik, S. S., Worden, J. R., Wofsy, S. C., Biraud, S. C., Nassar, R., Jones, D. B. A., Olsen, E.
28 T., Jiménez, R., Park, S., Santoni, G. W., Daube, B. C., Pittman, J. V., Stephens, B. B., Kort, E.
29 A., Osterman, G. B. TES team: Comparison of improved Aura Tropospheric Emission
30 Spectrometer CO₂ with HIPPO and SGP aircraft profile measurements, *Atmospheric Chemistry*
31 *and Physics*, 13(6), 3205–3225, doi:10.5194/acp-13-3205-2013, 2013.
32
33 Lacour, J. L., Risi, C., Clarisse, L., Bony, S., Hurtmans, D., Clerbaux, C. and Coheur, P.-F.: Mid-
34 tropospheric δD observations from IASI/MetOp at high spatial and temporal resolution,
35 *Atmospheric Chemistry and Physics*, 12(22), 10817–10832, doi:10.5194/acp-12-10817-2012,
36 2012.
37
38 Lacour, J.-L., Risi, C., Worden, J., Clerbaux, C. and Coheur, P.-F.: Importance of depth and
39 intensity of convection on the isotopic composition of water vapor as seen from IASI and TES δ
40 D observations, *Earth and Planetary Science Letters*, 481, 387–394,
41 doi:10.1016/j.epsl.2017.10.048, 2018.
42
43 Lamouroux, J., Régalia, L., Thomas, X., Vander Auwera, J., Gamache, R. R., Hartmann, J.-M.:
44 CO₂ line-mixing database and software update and its tests in the 2.1 μm and 4.3 μm regions,
45 *Journal Quantitative Spectroscopy Radiative Transfer*, 151, 88-96, 2015
46

1 Luo, M., Rinsland, C. P., Rodgers, C. D., Logan, J. A., Worden, H., Kulawik, S., Eldering, A.,
2 Goldman, A., Shephard, M. W., Gunson, M. and Lampel, M.: Comparison of carbon monoxide
3 measurements by TES and MOPITT: Influence of a priori data and instrument characteristics on
4 nadir atmospheric species retrievals, *Journal of Geophysical Research-Atmospheres* , 112(D9),
5 D09303, doi:10.1029/2006JD007663, 2007.
6
7 Moncet, J-L., G. Uymin, A. E. Lipton, and H. E. Snell: Infrared radiance modeling by optimal
8 spectral sampling. *J. Atmos. Sci.*, 65, 3917–3934, doi: 10.1175/2008JAS2711.1, 2008
9
10 Moncet, J-L., Uymin, G., Liang, P. and Lipton, A.E: Fast and accurate radiative transfer in the
11 thermal regime by simultaneous optimal spectral sampling over all channels. *Journal of the*
12 *Atmospheric Sciences*, vol 72, 2622-2641, doi: 0.1175/JAS-D-14-0190.1, 2015

13 Noone, D., Galewsky, J., Sharp, Z. D., Worden, J., Barnes, J., Baer, D., Bailey, A., Brown, D. P.,
14 Christensen, L., Crosson, E., Dong, F., Hurley, J. V., Johnson, L. R., Strong, M., Toohey, D.,
15 Van Pelt, A. and Wright, J. S.: Properties of air mass mixing and humidity in the subtropics from
16 measurements of the D/H isotope ratio of water vapor at the Mauna Loa Observatory, *Journal*
17 *Geophysical Research-Atmospheres*, 116(D22), D22113, doi:10.1029/2011JD015773, 2011.

18 Pagano, T. S., Aumann, H. H., Hagan, D. E., and Overoye, K.: Prelaunch and in-flight
19 radiometric calibration of the Atmospheric Infrared Sounder (AIRS), *IEEE Transactions on*
20 *Geoscience and Remote Sensing*, 41, 265–273, 2003.

21 Pagano, T. S., Aumann, H. H., Schindler, R., Elliott, D., Broberg, S., Overoye, K., and Weiler, M. H.:
22 Absolute radiometric calibration accuracy of the Atmospheric Infrared Sounder (AIRS), in: *Proc.*
23 *SPIE*, vol. 7081, doi:10.1117/12.795445, 2008.

24 Payne, V. H., Alvarado, M. J., Cady-Pereira, K. E., Worden, J. R., Kulawik, S. S. and Fischer, E.
25 V.: Satellite observations of peroxyacetyl nitrate from the Aura Tropospheric Emission
26 Spectrometer, *Atmospheric Measurement Techniques*, 7(11), 3737–3749, doi:10.5194/amt-7-
27 3737-2014, 2014.
28
29 Rodgers, C. D. and Connor, B. J.: Intercomparison of remote sounding instruments, *Journal of*
30 *Geophysical Research-Atmospheres*, 108, 4116, doi:10.1029/2002JD002299, 2003.
31
32 Risi, C., Noone, D., Worden, J., Frankenberg, C., Stiller, G., Kiefer, M., Funke, B., Walker, K.,
33 Bernath, P., Schneider, M., Wunch, D., Sherlock, V., Deutscher, N., Griffith, D., Wennberg, P.
34 O., Strong, K., Smale, D., Mahieu, E., Barthlott, S., Hase, F., García, O., Notholt, J., Warneke,
35 T., Toon, G., Sayres, D., Bony, S., Lee, J., Brown, D., Uemura, R. and Sturm, C.: Process-
36 evaluation of tropospheric humidity simulated by general circulation models using water vapor
37 isotopologues: 1. Comparison between models and observations, *Journal of Geophysical*
38 *Research-Atmospheres* , 117(D5), D05303, doi:10.1029/2011JD016621, 2012.
39
40 Risi, C., Noone, D., Frankenberg, C. and Worden, J.: Role of continental recycling in
41 intraseasonal variations of continental moisture as deduced from model simulations and water

1 vapor isotopic measurements, *Water Resour. Res.*, 49(7), 4136–4156, doi:10.1002/wrcr.20312,
2 2013.

3

4 Rothman, L. S., I. E. Gordon, Y. Babikov et al., "The HITRAN 2012 Molecular Spectroscopic
5 Database", *Journal of Quantitative Spectroscopy and Radiative Transfer* **130**, 4-50 (2013)
6

7 Schneider, M., Barthlott, S., Hase, F., González, Y., Yoshimura, K., García, O. E., Sepúlveda, E.,
8 Gomez-Pelaez, A., Gisi, M., Kohlhepp, R., Dohe, S., Blumenstock, T., Wiecele, A., Christner,
9 E., Strong, K., Weaver, D., Palm, M., Deutscher, N. M., Warneke, T., Notholt, J., Lejeune, B.,
10 Demoulin, P., Jones, N., Griffith, D. W. T., Smale, D. and Robinson, J.: Ground-based remote
11 sensing of tropospheric water vapour isotopologues within the project MUSICA, *Atmospheric
12 Measurement Techniques* , 5(12), 3007–3027, doi:10.5194/amt-5-3007-2012, 2012.
13

14 Shephard, M. W., Worden, H. M., Cady-Pereira, K. E., Lampel, M., Luo, M., Bowman, K. W.,
15 Sarkissian, E., Beer, R., Rider, D. M., Tobin, D. C., Revercomb, H. E., Fisher, B. M., Tremblay,
16 D., Clough, S. A., Osterman, G. B. and Gunson, M.: Tropospheric Emission Spectrometer nadir
17 spectral radiance comparisons, *Journal of Geophysical Research-Atmospheres* , 113(D15),
18 D15S05, doi:10.1029/2007JD008856, 2008.
19

20 Shephard, M. W. and Cady-Pereira, K. E.: Cross-track Infrared Sounder (CrIS) satellite
21 observations of tropospheric ammonia, *Atmospheric Measurement Techniques*, 8(3), 1323–1336,
22 doi:10.5194/acpd-15-4823-2015, 2015.

23 Strow, L. L., Hannon, S., Weiler, M., Overoye, K., Gaiser, S. L., Aumann, H. H.: Prelaunch
24 spectral calibration of the atmospheric infrared sounder (AIRS), *IEEE Transactions Geoscience
25 and Remote Sensing*, 41(2), 274-286, doi: 10.1109/TGRS.2002.808245, 2003
26

27 Tran, H., Flaud J-M, Gabard, T., Hase, F., Von Clarmann, T., Camy-Peyret, C., Payan, S.,
28 Hartmann, J-M.: Model, software, and database for line-mixing effects in the n_3 and n_2 bands of
29 CH₄ and tests using laboratory and planetary measurements. I. N₂ (and air) broadenings and the
30 Earth atmosphere, *Journal Quantitative Spectroscopy Radiative Transfer*, 101, 284-305, 2006
31

32 Worden, J., Kulawik, S., Shepard, M., Clough, S., Worden, H., Bowman, K. and Goldman, A.:
33 Predicted errors of tropospheric emission spectrometer nadir retrievals from spectral window
34 selection, *Journal of Geophysical Research-Atmospheres*, 109(D9), D09308,
35 doi:10.1029/2004JD004522, 2004.
36

37 Worden, J., Bowman, K., Noone, D., Beer, R., Clough, S., Eldering, A., Fisher, B., Goldman, A.,
38 Gunson, M., Herman, R., Kulawik, S. S., Lampel, M., Luo, M., Osterman, G., Rinsland, C.,
39 Rodgers, C., Sander, S., Shephard, M. and Worden, H.: Tropospheric Emission Spectrometer
40 observations of the tropospheric HDO/H₂O ratio: Estimation approach and characterization,
41 *Journal of Geophysical Research-Atmospheres* , 111(D16), doi:10.1029/2005JD006606, 2006.
42

43 Worden, J., Noone, D., Bowman, K., Beer, R., Eldering, A., Fisher, B., Gunson, M., Goldman,
44 A., Herman, R., Kulawik, S. S., Lampel, M., Osterman, G., Rinsland, C., Rodgers, C., Sander,
45 S., Shephard, M., Webster, C. R. and Worden, H.: Importance of rain evaporation and

1 continental convection in the tropical water cycle, *Nature*, 445(7127), 528–532,
2 doi:10.1038/nature05508, 2007a.
3
4 Worden, J., D. Noone, J. Galewsky, A. Bailey, K. Bowman, D. Brown, J. Hurley, S. Kulawik, J.
5 Lee, and M. Strong (2011), Estimate of bias in Aura TES HDO/H₂O profiles from comparison
6 of TES and in situ HDO/H₂O measurements at the Mauna Loa observatory, *Atmospheric*
7 *Chemistry and Physics*, 11(9), 4491–4503, doi:10.5194/acp-11-4491-2011.
8
9 Worden, J., Kulawik, S., Frankenberg, C., Payne, V., Bowman, K., Cady-Peirara, K., Wecht, K.,
10 Lee, J.-E. and Noone, D.: Profiles of CH₄, HDO, H₂O, and N₂O with improved lower
11 tropospheric vertical resolution from Aura TES radiances, *Atmospheric Measurement*
12 *Techniques*, 5(2), 397–411, doi:10.5194/amt-5-397-2012, 2012.
13
14 Worden, J., Wecht, K., Frankenberg, C., Alvarado, M., Bowman, K., Kort, E., Kulawik, S., Lee,
15 M., Payne, V. and Worden, H.: CH₄ and CO distributions over tropical fires during October
16 2006 observed by the Aura TES satellite instrument and modeled by GEOS-Chem, *Atmospheric*
17 *Chemistry and Physics*, 13(7), 3679–3692, doi:10.5194/acp-13-3679-2013, 2013.
18
19 Worden, J. R., Turner, A. J., Bloom, A., Kulawik, S. S., Liu, J., Lee, M., Weidner, R., Bowman,
20 K., Frankenberg, C., Parker, R. and Payne, V. H.: Quantifying lower tropospheric methane
21 concentrations using GOSAT near-IR and TES thermal IR measurements, *Atmospheric*
22 *Measurement Techniques*, 8(8), 3433–3445, doi:10.5194/amt-8-3433-2015, 2015.
23
24 Wright, J. S., Fu, R., Worden, J. R., Chakraborty, S., Clinton, N., Risi, C., sun, Y. and Yin, L.:
25 Rainforest-initiated wet season onset over the southern Amazon, *Proceedings of the National*
26 *academy of Sciences*, 1–6, doi:10.1073/pnas.1621516114/-/DCSupplemental, 2017.
27
28 Xiong, X., Barnet, C., Maddy, E., Sweeney, C., Liu, X., Zhou, L. and Goldberg, M.:
29 Characterization and validation of methane products from the Atmospheric Infrared Sounder
30 (AIRS), *Journal Geophysical Research-Biogeosciences*, 113, doi:10.1029/2007JG000500, 2008.
31
32 Xiong, X., Barnet, C., Maddy, E., Wofsy, S. C., Chen, L. A., Karion, A. and Sweeney, C.:
33 Detection of methane depletion associated with stratospheric intrusion by atmospheric infrared
34 sounder (AIRS), *Geophysical Research Letters*, 40(10), 2455–2459, doi:10.1002/grl.50476,
35 2013.
36
37 Xiong, X., Barnet, C., Maddy, E., Sweeney, C., Liu, X., Zhou, L. and Goldberg, M.:
38 Characterization and validation of methane products from the Atmospheric Infrared Sounder
39 (AIRS), *J. Geophys. Res.*, 113(null), G00A01, doi:10.1029/2007JG000500, 2008.
40
41 Zhou, L., Tian, Y., Myneni, R. B., Ciais, P., Saatchi, S., Liu, Y. Y., Piao, S., Chen, H., Vermote,
42 E. F., Song, C. and Hwang, T.: Widespread decline of Congo rainforest greenness in the past
43 decade, *Nature*, 508(7498), 86–90, doi:10.1038/nature13265, 2014.
44
45

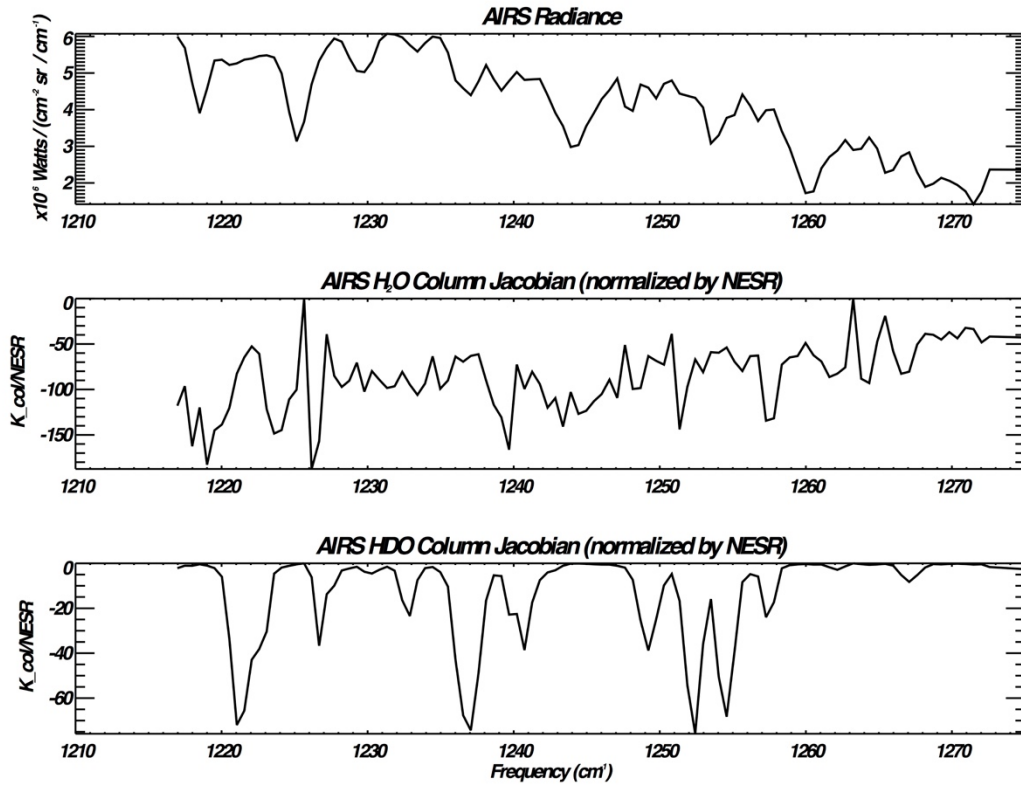
1 Table 1: Comparison between averaged TES and AIRS HDO/H₂O ratio (750-350 hPa). The units
2 are in parts per thousand relative to Standard Mean Ocean Water. The second column shows the
3 expected RMS based on the uncertainties of the TES and AIRS data. The third column shows the
4 actual RMS difference between TES and AIRS. The last column shows the mean difference.

| Date | Expected RMS (per mil / SMOW) | Actual RMS (per mil / SMOW) | Mean (TES-AIRS) (per mil / SMOW) |
|------------|----------------------------------|--------------------------------|-------------------------------------|
| 2006-06-01 | 31.1 | 30.6 | -2.7 +/- 1.5 |
| 2007-06-02 | 30.0 | 31.9 | -0.6 +/- 1.5 |
| 2008-06-02 | 31.5 | 29.3 | 0.5 +/- 1.4 |
| 2009-07-06 | 31.6 | 27.1 | 0.7 +/- 1.4 |
| 2010-06-02 | 31.6 | 28.2 | 3.7 +/- 1.2 |

5

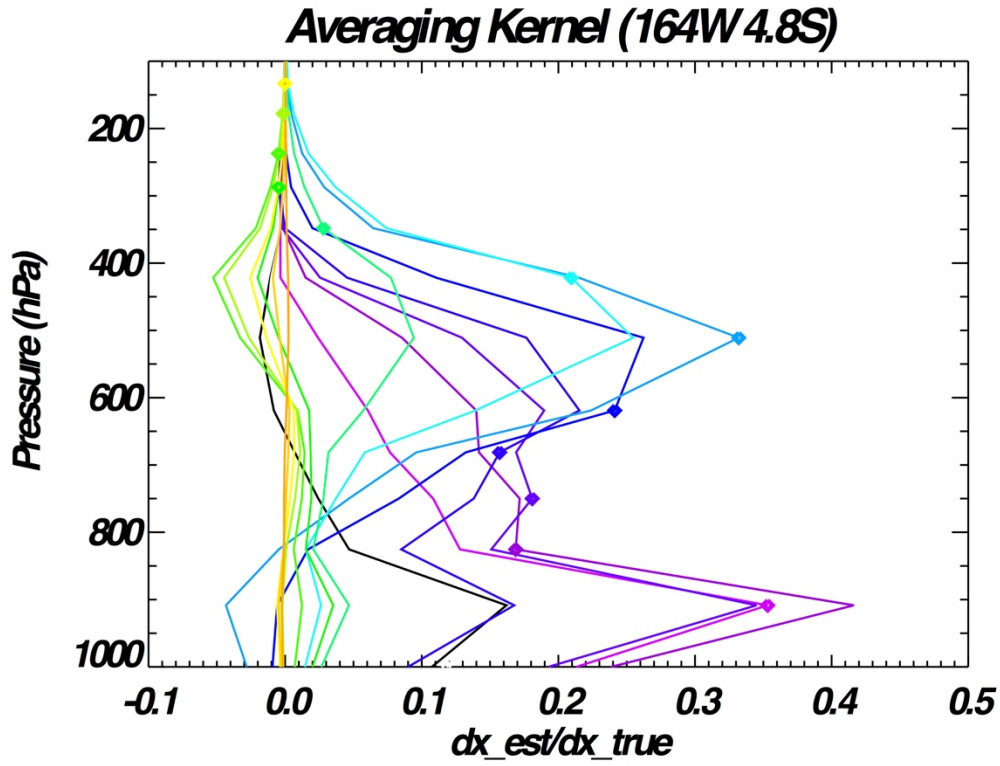
6

1
2



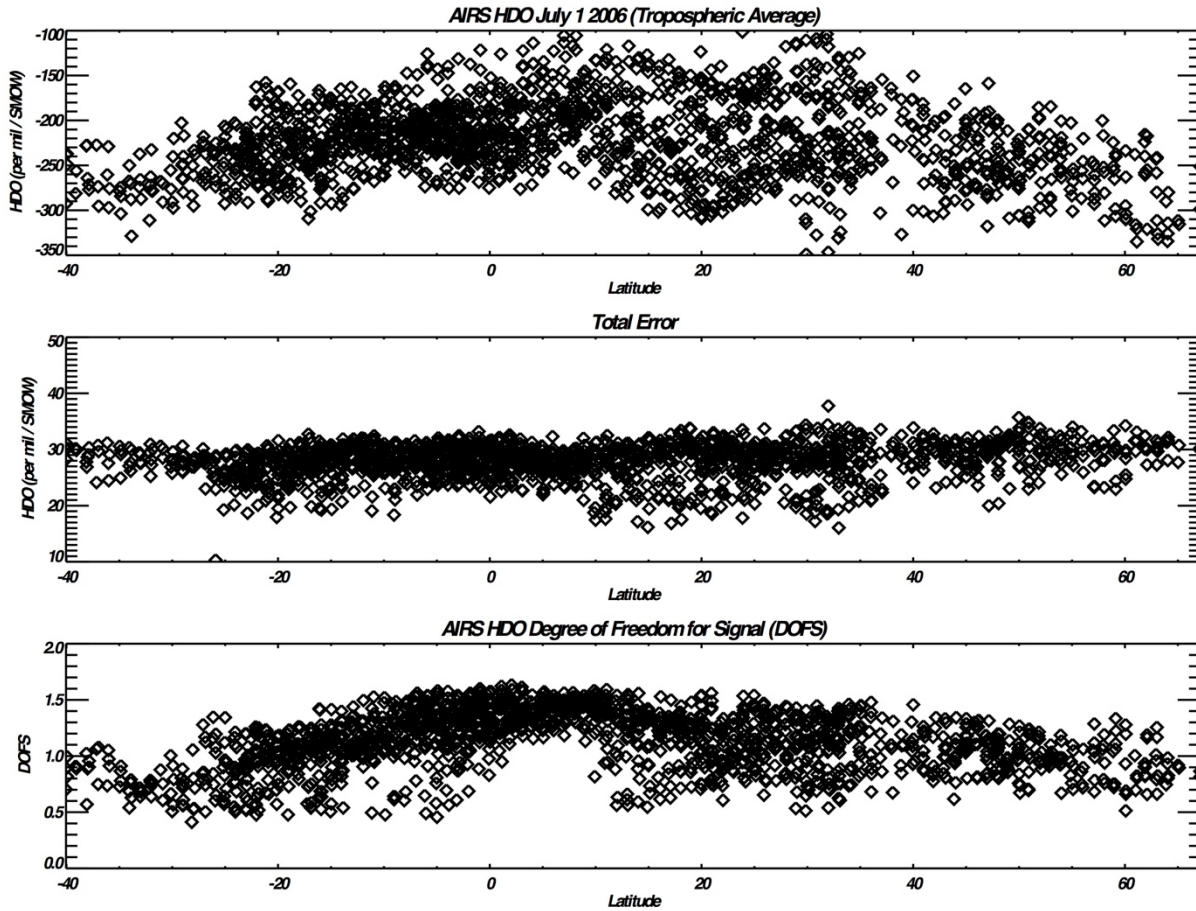
3
4 Figure 1: (top) AIRS radiance at approximately 8 microns for a typical tropical scene. (middle)
5 The total column (log) Jacobian for H₂O normalized by the AIRS NESR. (bottom) The total
6 column (log) Jacobian for HDO normalized by the AIRS NESR.

7
8



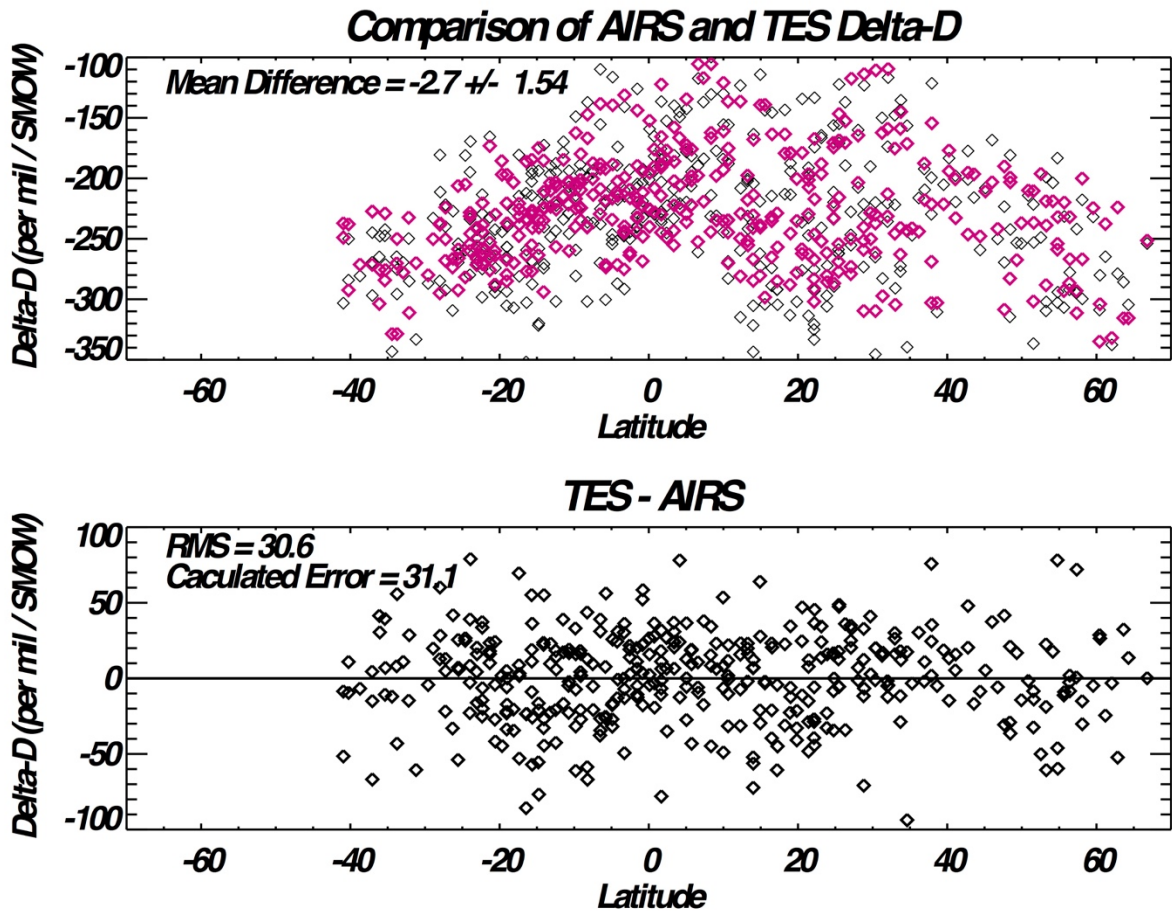
1
2
3
4
5
6
7

Figure 2: The rows of the averaging kernel matrix for the HDO retrieval corresponding to the radiance shown in Figure 1. The different colors and symbols are used to indicate the pressure levels corresponding to each row of the averaging kernel matrix.



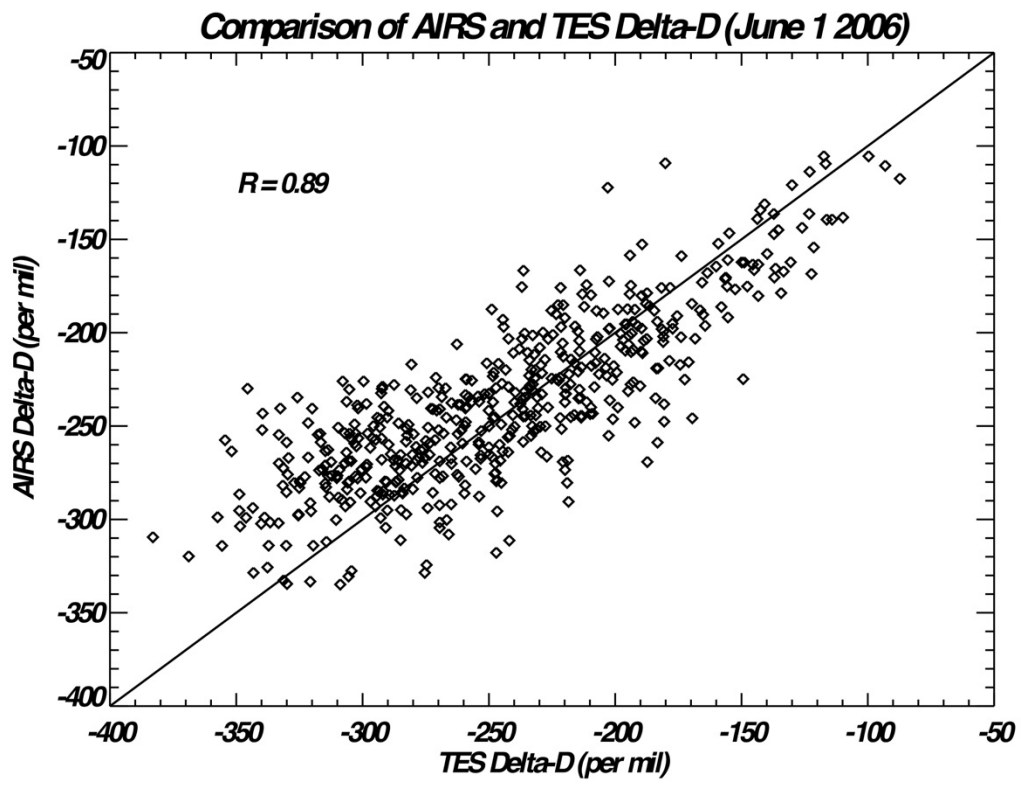
1
 2
 3 Figure 3: (top) The mean tropospheric deuterium content (in “per mil” or units of parts per
 4 thousand relative to the deuterium content of the ocean or SMOW) for June 1 2006 as inferred
 5 from AIRS radiance measurements. (middle) The total error for the measurements in the top
 6 panel (also in units of per mil relative to SMOW). (bottom) The DOFS for the retrieval.
 7
 8

1



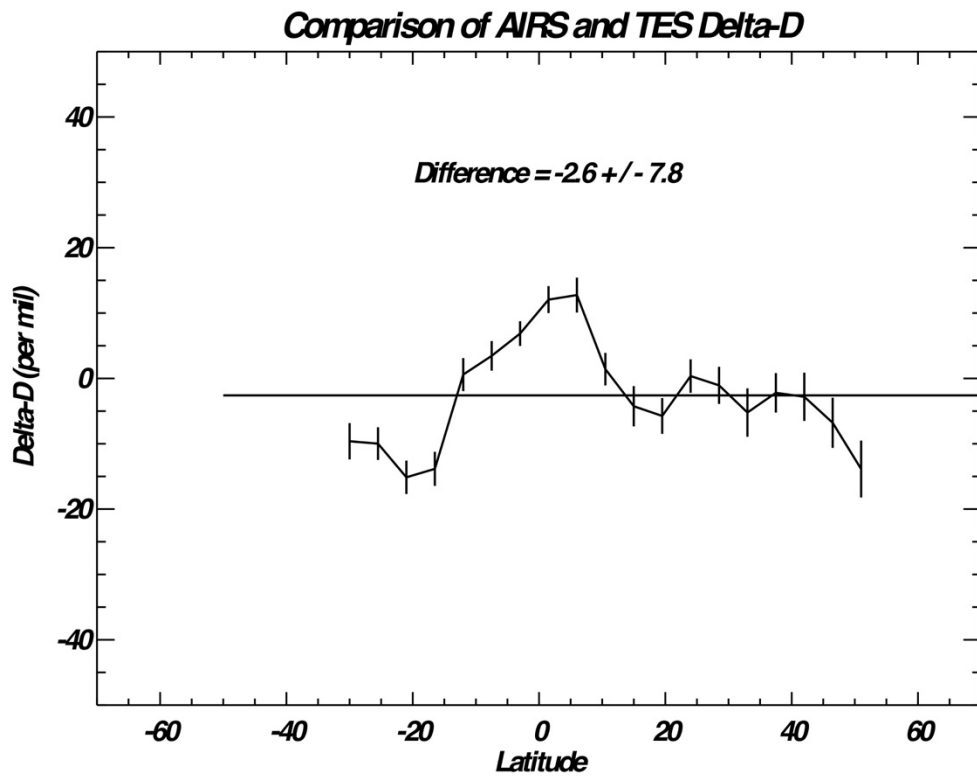
2
3
4
5
6

Figure 4: (top) Comparison of AIRS (red) and TES (black) delta-D for June 1 2006 (~600 co-located observations). (bottom) The differences (after bias subtraction) between TES and AIRS delta-D measurements.



1
2 Figure 5: Comparison of the AIRS and TES deuterium content. The solid line is the one-to-one
3 line.
4
5
6

1



2
3 Figure 6: The Latitudinal differences between TES and AIRS Delta-D using co-located
4 observations for 5 days (approximately 600 observations per day) of data, spaced over 5
5 Northern Hemisphere summers between 2006 and 2010.
6